Phase and amplitude of element-specific moment precession in $Ni_{81}Fe_{19}$

Y. Guan and W. E. Bailey

Materials Science Program, Department of Applied Physics,

Columbia University, New York, New York 10027

E. Vescovo, C.-C. Kao, and D. A. Arena

National Synchrotron Light Source,

Brookhaven National Laboratory, Upton, New York 11973

(Dated: October 27, 2006)

Abstract

We present a time and element-resolved measurement of magnetization dynamics during ferromagnetic resonance (FMR) in a single layer of $Ni_{81}Fe_{19}$. Small-angle ($<1^{\circ}$) precession of elemental Ni, Fe moments could be measured directly and quantitatively using time-resolved x-ray magnetic circular dichroism (XMCD) in transmission. The high temporal and rotational sensitivity of this technique has allowed quantification of the phase and amplitude of driven FMR motion at 2.3 GHz, verifying basic expectations for a driven resonance.

PACS numbers: 76.50.+g, 76.90.+d, 78.70.CK

Keywords: ferromagnetic alloy, ferromagnetic resonance, magnetization dynamics, time-resolved XMCD

INTRODUCTION

Ferromagnetic resonance (FMR) is a venerable topic in the study of magnetism. In the modern technological context, resonance and relaxation underpin the switching response of spin electronic devices at 1 GHz and above. Materials-based techniques to engineer the high-speed response, through dopant-based control of relaxation, beg the question of the *microscopic* roles of the dopants, and degree of coupling between them.

In this Letter, we demonstrate a time- and element-resolved measurement of ferromagnetic resonance in a single layer of $Ni_{81}Fe_{19}$. Conventional, low-angle ($\sim$ 0.1-1.0°) FMR motion, driven with a continuous wave (CW) low-power microwave field at 2.3 GHz, has been measured in the time-domain using time-resolved x-ray magnetic circular dichroism (XMCD). Temporal resolution is demonstrated to ± 2 ps and rotational resolution to $\pm 0.1°$, both an order of magnitude better than demonstrated in previous element-specific precession measurements[1]. Quantitative measurement of phase and amplitude are validated through comparison with a single-domain forced oscillator model.

Two innovations have allowed the rotational and spatial resolution necessary for the measurement. High magnetic contrast is provided by transmission geometry XMCD[2, 3], the soft x-ray equivalent of Faraday rotation. Improved temporal resolution is provided using phase-locked CW microwaves as an excitation source, suppressing the effects of timing jitter present in pulsed experiments[1].

THEORY

In general, magnetization dynamics are described by the Landau-Lifshitz (LL) equation[4], given in SI as

$$\frac{d\mathbf{M}}{dt} = -\mu_0 \mid \gamma \mid (\mathbf{M} \times \mathbf{H}) - \frac{\lambda}{M_s^2} (\mathbf{M} \times \mathbf{M} \times \mathbf{H}), \tag{1}$$

where λ is the LL relaxation rate in $\sec^{-1}$.

The LL equation can be linearized for small rotations of $\vec{M}$ about $\vec{H}$ as

$$\frac{\partial^2 \phi(t)}{\partial t^2} + \lambda \frac{\partial \phi(t)}{\partial t} + \omega_0^2 \phi(t) = 0, \tag{2}$$

where $\omega_0^2 = \mu_0^2 \gamma^2 H_{eff}(H_{eff} + M_s)$ [5].

Free oscillations, describing the motion of this damped harmonic oscillator about an equilibrium position, are the starting point for most relevant magnetooptical studies of spin

dynamics[1, 6–8]. Rotational displacements about an equilibrium are described by ϕ; ω_0 is is the circular frequency of ferromagnetic resonance (FMR) and $2/\lambda$ is its characteristic relaxation time.

If instead the motion is forced by a transverse ac field $H_y(t) = H_{y0}\exp(i\omega t)$, the response is given as

$$\frac{\partial^2\phi(t)}{\partial t^2} + \lambda\frac{\partial\phi(t)}{\partial t} + \omega_0^2\phi(t) = A\exp(i\omega t), \tag{3}$$

where $A \approx \mu_0^2\gamma^2 M_s H_{y0}$. Solving Eq. (3) using $\phi(t) = \phi_0\exp(i\omega t) =\mid \phi_0 \mid \exp[i(\omega t+\delta)]$, then

$$\phi_0 = \frac{A}{(\omega_0^2-\omega^2)^2+\lambda^2\omega^2}[(\omega_0^2-\omega^2) - i\omega\lambda]. \tag{4}$$

Thus, the phase δ and the amplitude of driven FMR precession can be expressed as:

$$\tan\delta = \frac{-\lambda\omega}{\omega_0^2-\omega^2}, \tag{5}$$

$$\mid \phi_0 \mid = \frac{A}{\sqrt{(\omega_0^2-\omega^2)^2+\lambda^2\omega^2}}. \tag{6}$$

These relationships can now be tested directly. Moreover, using *in-situ* FMR (microwave absorption) measurement, the damping λ can be estimated directly through the field linewidth, allowing for a parameter-free comparison with Eqs. (5) and (6).

FMR absorption is given by the imaginary part of the susceptibility, $\chi^{''}$, along the rf driving field, H_y, according to Eq. (4). The field-swept resonance linewidth has half-power points at $\mu_0\Delta H_{1/2} = 2\alpha\omega/\gamma$, directly proportional to the dimensionless damping constant α. Between these half-power points, the phase lag δ of $\phi(t)$ with respect to the drive field goes through a change of 90° according to Eq. (5).

In lock-in (derivative) detection of microwave absorption, the inflection points of the Lorenzian line shape are more easily seen. These have a width $\mu_0\Delta H_{pp} = (2/\sqrt{3})\alpha\omega/\gamma$[9]. While $\alpha = \lambda/(\mu_0 M_s\gamma)$ for low damping ($\alpha \ll 1$), λ can thus be expressed as

$$\lambda = \frac{\sqrt{3}}{2}\frac{\mu_0^2\gamma^2 M_s\Delta H_{pp}}{\omega}. \tag{7}$$

Then, the following relationship can be derived as

$$\sqrt{3}\Delta H_{pp} = \Delta H_{1/2} = \frac{1}{\sqrt{3}}\Delta H_{\frac{1}{2}|\phi_0|}, \tag{8}$$

where $\Delta H_{\frac{1}{2}|\phi_0|}$ denotes the linewidth defined by the half-amplitude points.

EXPERIMENT

Time-resolved XMCD (TR-XMCD) measurements of magnetization motion during FMR precession were carried out at Beamline 4-ID-C of Advanced Photon Source in Argonne, IL. The circular dichroism signal was obtained in transmission, using photon helicity $\vec{\sigma}$ switching ($\vec{\sigma}$, with an incident angle of 38° from normal, and with in-plane projection along $\hat{\mathbf{y}}$) at the elliptical undulator for fixed static applied field H_B. The transmitted intensity was read at a soft x-ray sensitive photodiode and normalized to an incident intensity at a reference grid.

Transmission measurements require an x-ray transparent sample and substrate. For time-resolved measurements, x-ray transparent RF field delivery system is also necessary. The $Ni_{81}Fe_{19}$(25nm)/Cu(2nm) thin film sample was deposited onto a commercially available, supported Si_3N_4 membrane window (1.0 mm square and 100 nm thick) using UHV magnetron sputtering at a base pressure of 4×10^{-9} Torr. Transmission through the substrate is greater than 80% at the transition metal edges of interest. The spot size of the photon beam ($\sim$ 100 μm $\times$ 50μm) is smaller than the lateral size of the membrane window. The sample was placed in the center of a hollow microwave resonator. Uniform precession of the magnetization was excited at 2.3 GHz by a CW low-power microwave field, synchronized with variable delay to APS x-ray photon bunches (88 MHz). The measurement technique bears some similarity with the time-resolved MOKE-FMR technique presented in Ref. [8], but XMCD substitutes element specificity for the spatial resolution in that work. Microwave absorption was measured *in-situ*, using standard lock-in techniques, detecting reflected power at the resonator. Orthogonal Helmholtz coils were used to apply longitudinal bias field $H_B\hat{\mathbf{x}}$ or transverse bias field $H_T\hat{\mathbf{y}}$.

Element-specific XMCD hysteresis loops were taken as a function of transverse bias field H_T to obtain a calibration for magnetization angle ϕ. Photon energies were set to the L_3 peaks for Fe (707.5 eV) and Ni (852.0 eV) to measure Fe and Ni XMCD signals, respectively. The saturation values of XMCD signals are taken to be $\phi_{Fe} = \phi_{Ni} = \pm 90°$.

RESULTS AND DISCUSSION

$L_{2,3}$-edge XAS and MCD spectra have been measured in transmission for both Fe and Ni in $Ni_{81}Fe_{19}$. High-quality spectra are obtained here, as shown in our previous work at NSLS, Beamline U4B[3]. Fig. 1(a) shows Fe transmission XAS spectra for both photon helicity directions, with the difference. Corresponding spectra for Ni are shown in Fig. 1(b).

Time- and element-resolved XMCD measurements of magnetization precession at resonance are presented in Fig. 2. XMCD signals were taken as a function of delay time and converted into time-dependent elemental magnetization angles $\phi_{Fe}(t)$ and $\phi_{Ni}(t)$ for Fe and Ni, respectively[1]. Precessional oscillations are clearly seen.

Use of CW microwave excitation source is effective in averaging any timing jitter or finite temporal width. For a sinusoidal wave, all points can be weighted equally in temporal (phase) resolution, so for N sampling points, the phase resolution can be improved by a factor $\sqrt{N}$. For the roughly 100 sampling points on e.g. Fig. 3, this improves the temporal (phase) resolution by an order of magnitude to the few ps range; errors in sinusoidal fits are in this range. Our Fe and Ni time traces are coupled within ± 2 ps in time, so this is taken as the approximate temporal resolution, an order of magnitude smaller than the intrinsic bunch width of the x-ray photons ($\sim$ 60 ps FWHM). In addition, Fe and Ni moments are coupled within $\pm 0.1^\circ$ in precessional cone angle.

Time-resolved XMCD measurements of magnetization precession off resonance are presented in Fig. 3. Applied fields were selected according to *in-situ* measured FMR spectra (Fig. 4(a)), spanning the resonance condition H_{res} (37 Oe) to $\sim 4 \times \Delta H_{pp}$ off resonance (5 Oe). A clear variation in the amplitude of driven FMR motion $\phi_{Fe}(t)$, and its phase, compared with the RF excitation field, can be seen.

The key result of this letter is presented in Fig. 4(b). Verifying basic expectations of a driven resonance, we can clearly see a 90° phase shift generated through the adjustment of ω_0 (through longitudinal bias field H_B) to $\ll \omega$, and a Lorentzian variation of the precessional amplitude. Both behaviors are in excellent agreement with the linearized model (Eqs. (5) and (6)). No empirical parameters have been used apart from H_{y0}. The relaxation rate $\lambda/4\pi$ is estimated as 140 MHz $\pm$ 10 MHz directly from the *in-situ* measured FMR spectra (Fig. 4(a)) using Eq. (7), which is in reasonable agreement with those found by conventional FMR measurements($\sim$ 120 MHz)[10, 11], or by pulsed inductive microwave magnetometer (PIMM) measurements in a similar field/frequency range (140-150 MHz)[12]; the single frequency measurement of $\lambda/4\pi$ here and in PIMM contains a small unknown inhomogeneous contribution (ΔH_0), which will tend to raise estimates of $\lambda/4\pi$ at low frequencies. In addition, we verify directly the relationship in Eq. (8), with $\sqrt{3}$ separating the peak-to-peak, 1/2 power (90° phase shift), and 1/2 amplitude linewidths.

The measurement clearly opens the possibility for direct tests of microscopic processes in relaxation (damping). Lagged phases between the precession of microscopic moments -

impurity and host moments for doped materials[13, 14] and spin and orbital moments for pure materials[15, 16] - are all posited for the origins of Gilbert damping. We can now claim the resolution in time (± 2 ps) and rotational angle ($<0.1^\circ$) very close to that needed to address these models directly.

CONCLUSION

We have measured driven ferromagnetic resonance (FMR) precession in the time domain using time-resolved XMCD. Precessional phase and amplitude, lumped together in microwave absorption measurement, could be measured directly, providing a vivid illustration of damped oscillator behavior.

ACKNOWLEDGEMENTS

The authors thank Carl Patton for a critical reading of this manuscript, and David J. Keavney (APS) for beamline support. This work was partially supported by the Army Research Office with Grant No. ARO-43986-MS-YIP, and the National Science Foundation with Grant No. NSF-DMR-02-39724. Use of the Advanced Photon Source was supported by the U.S. Department of Energy, Office of Science, Office of Basic Energy Sciences, under Contract No. W-31-109-Eng-38.

REFERENCES

[1] W. E. Bailey, L. Cheng, D. J. Keavney, C. -C. kao, E. Vescovo, and D. A. Arena, Phys. Rev. B **70**, 172403 (2004).

[2] C. Chen, Y. Idzerda, H.-J. Lin, N. Smith, G. Meigs, E. Chaban, G. Ho, E. Pellegrin, and F. Sette, Phys. Rev. Lett. **75**, 152 (1995).

[3] Y. Guan, Z. Dios, D. A. Arena, L. Cheng, and W. E. Bailey, J. Appl. Phys. **97**, 10A719 (2005).

[4] L. D. Landau, E. M. Lifshitz, and L. P. Pitaevski, *Statistical Physics, Part 2* (Pergamon, Oxford, 1980).

[5] Charles Kittel, *Introduction to Solid State Physics* (Wiley, 2005)

[6] D. M. Engebretson, J. Berezovsky, J. P. Park, L. C. Chen, C. J. Palmstrom, and P. A. Crowell, J. Appl. Phys. **91**, 8040 (2002).

[7] R. Meckenstock, M. Möller, and D. Spoddig, Appl. Phys. Lett. **86**, 112506 (2005).

[8] S. Tamaru, J. A. Bain, R. J. M. van de Veerdonk, T. M. Crawford, M. Covington, and M. H. Kryder, Phys. Rev. B **70**, 104416 (2004).

[9] B. Heinrich, *Ultrathin Magnetic Structures II*, edited by B. Heinrich and J. A. C. Bland (Springer-Verlag, Berlin, 1994).

[10] D. J. Twisselmann, and R. D. McMichael, J. Appl. Phys. **93**, 6903 (2003).

[11] V. Dasgupta, N. Litombe, W. E. Bailey, and H. Bakhru, J. Appl. Phys. **99**, 08G312 (2006).

[12] T. J. Silva, C. S. Lee, T. M. Crawford, and C. T. Rogers, J. Appl. Phys. **85**, 7849 (1999).

[13] P. -G. De Gennes, C. Kittel, and A. M. Portis, Phys. Rev. **116**, 323 (1959).

[14] B. H. Clarke, K. Tweedale, and R. W. Teale, Phys. Rev. **139**, A1933 (1965).

[15] V. Kamberský, Canadian J. Phys. **48**, 2906 (1970).

[16] J. Kuneš and V. Kamberský, Phys. Rev. B **65**, 212411 (2002).

Figures

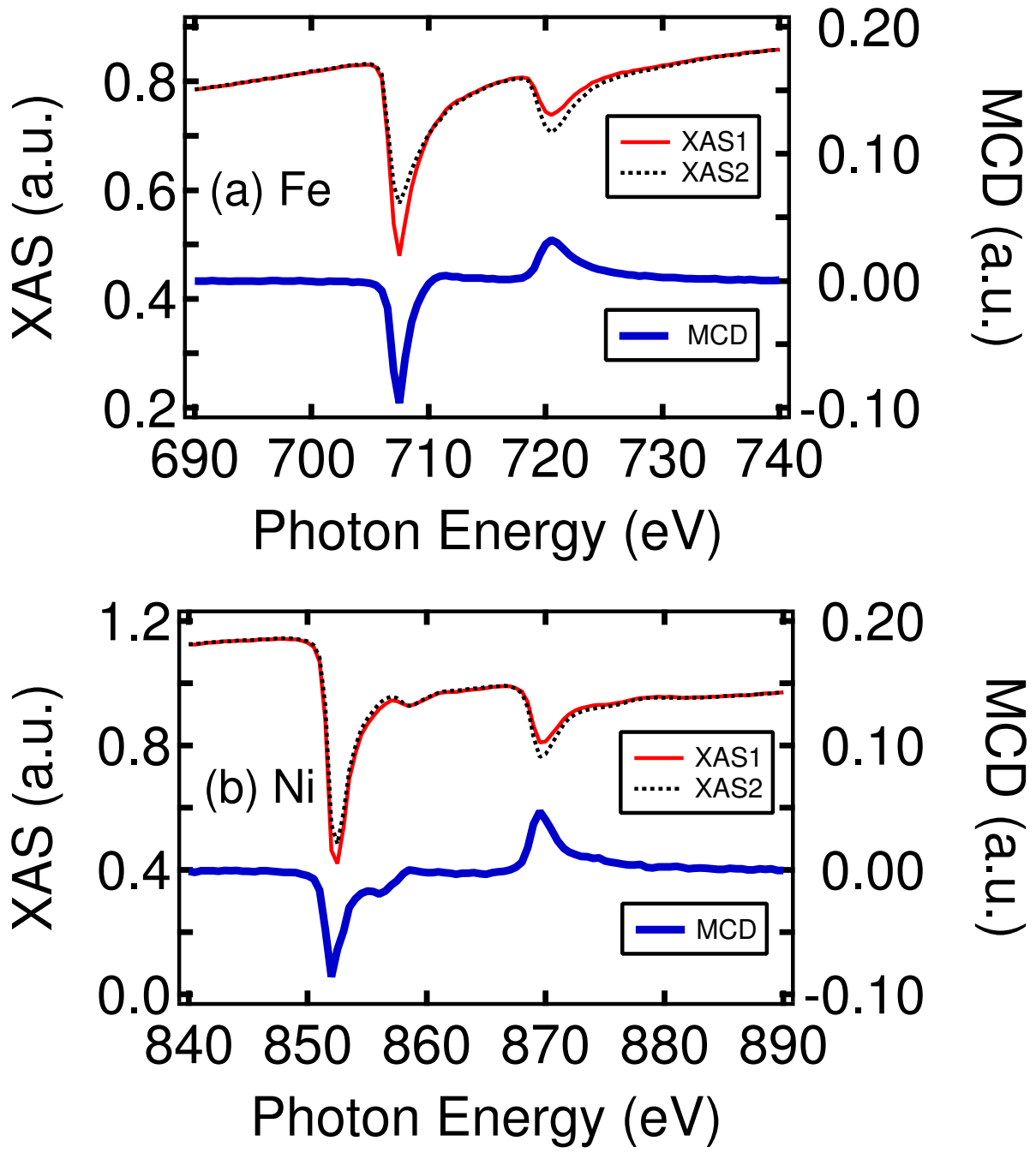

FIG. 1: (Color online)(a)$L_{2,3}$-edge transmission XAS and MCD spectra of Fe in $Ni_{81}Fe_{19}$;(b)$L_{2,3}$-edge transmission XAS and MCD spectra of Ni in $Ni_{81}Fe_{19}$.

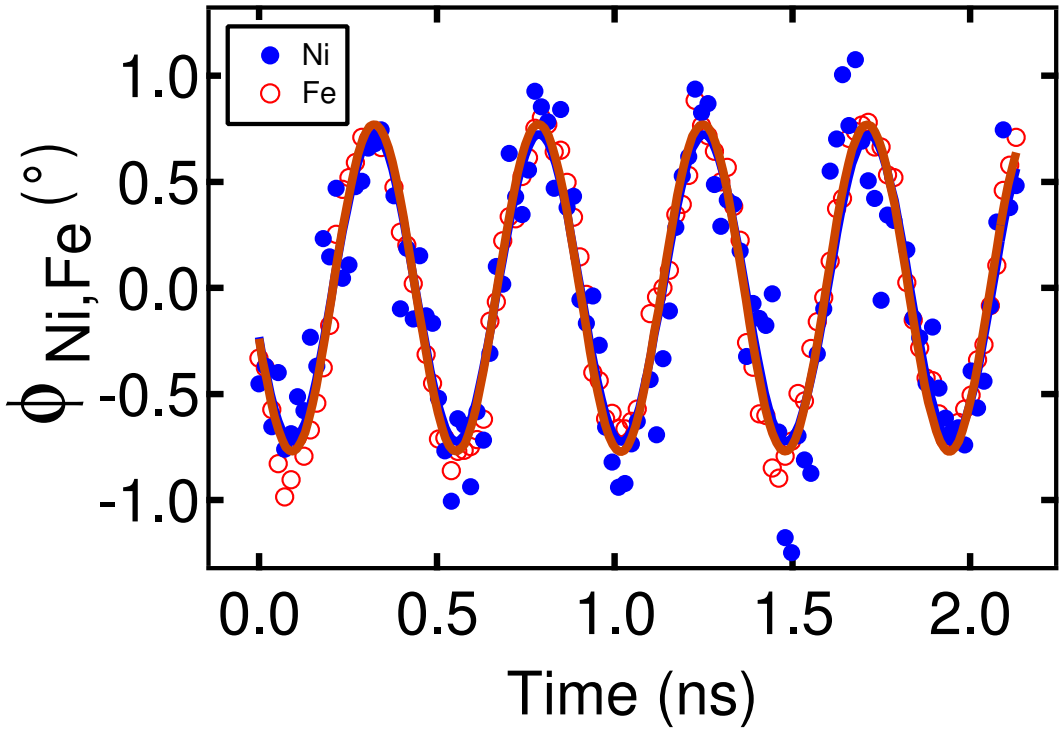

FIG. 2: (Color online)TR-XMCD measurement of Fe and Ni magnetization precession at resonance, 37 Oe at 2.3 GHz. Solid lines are sinusoidal fits of the Fe and Ni data sets separately.

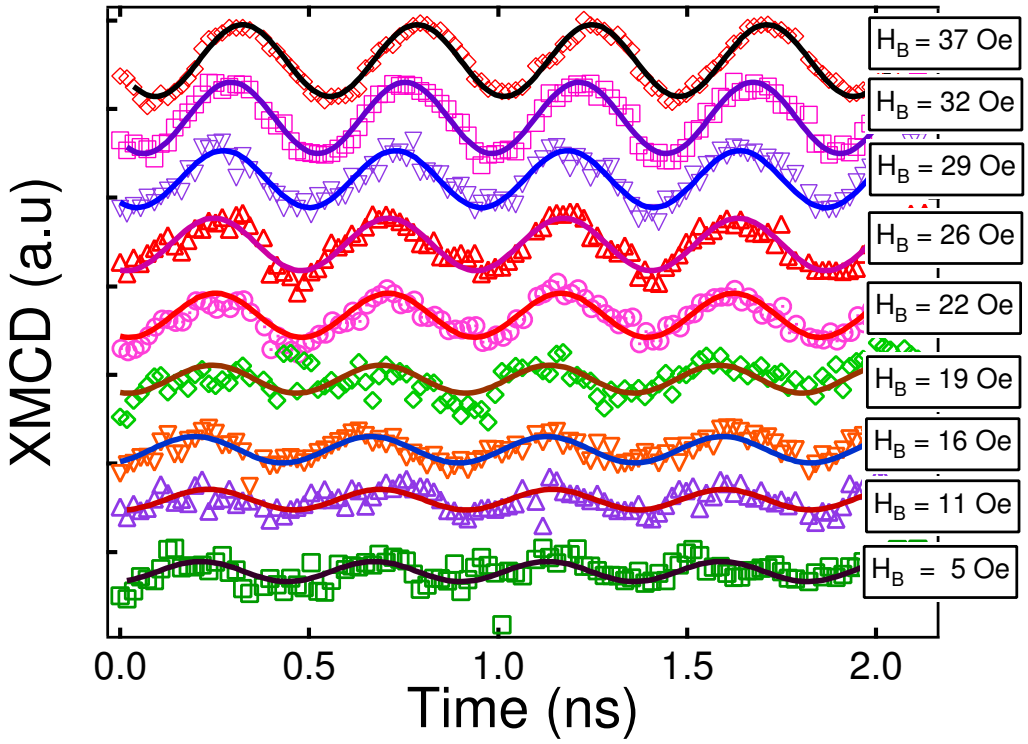

FIG. 3: (Color online)TR-XMCD measurement of $Ni_{81}Fe_{19}$ magnetization precession off resonance at Fe L_3 edge. Solid lines are sinusoidal fits.

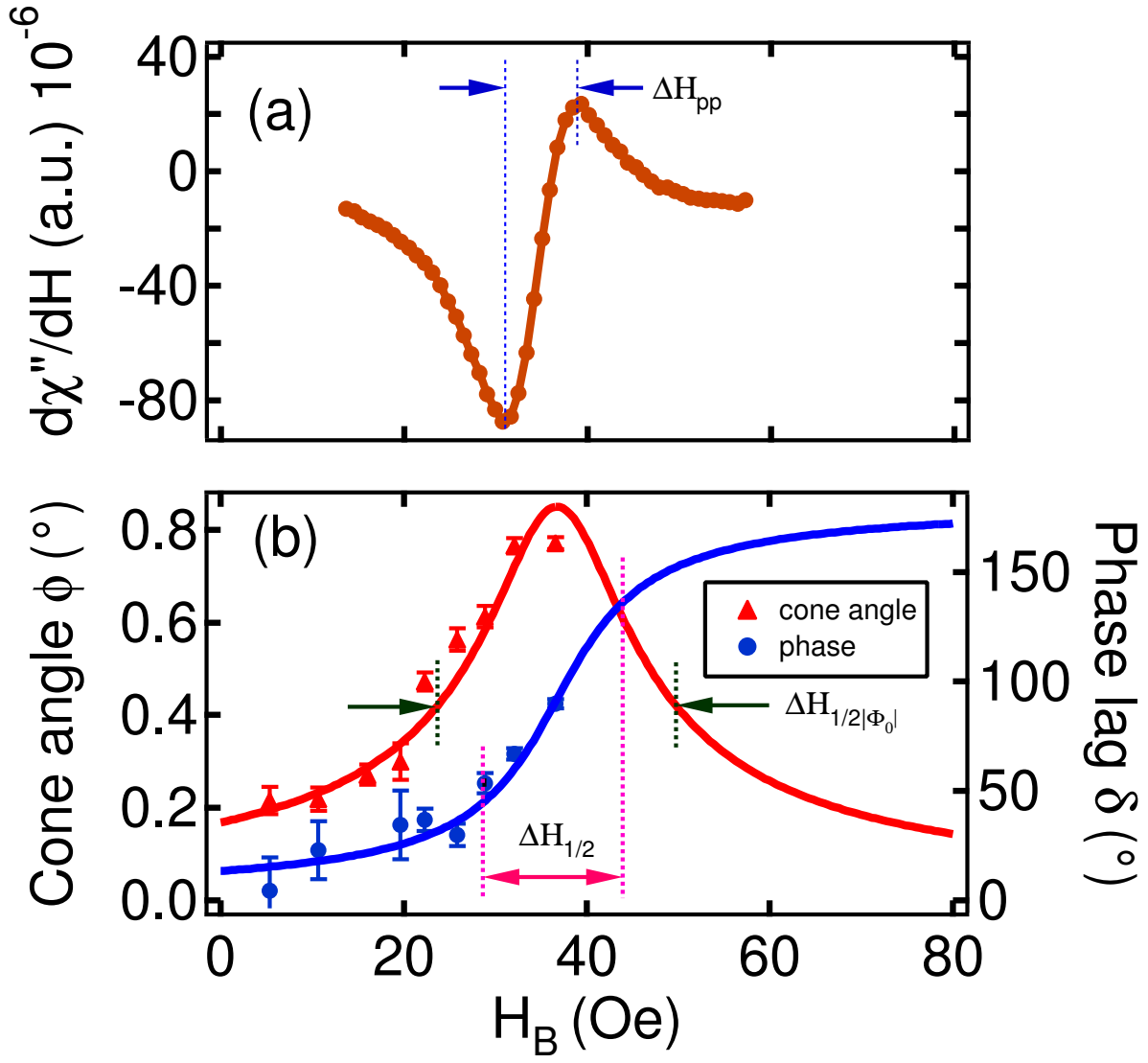

FIG. 4: (Color online)(a)*In-situ* measurement of FMR spectra of $Ni_{81}Fe_{19}$ by microwave absorption at 2.3 GHz; (b)Measurement of phase and amplitude of driven FMR precession in $Ni_{81}Fe_{19}$ by TR-XMCD. Solid lines are the corresponding theoretical simulations from Eqs. (5) and (6).